frontiers in Forests and Global Change

ORIGINAL RESEARCH
published: 04 February 2020
doi: 10.3389/ffgc.2020.00006

Short-Term Effects of Recent Fire on the Production and Translocation of Pyrogenic Carbon in Great Smoky Mountains National Park

Lauren M. Matosziuk[1], Adrian Gallo[1], Jeff Hatten[1], Kevin D. Bladon[1], Danica Ruud[1], Maggie Bowman[2], Jessica Egan[2], Kate Heckman[3], Michael SanClements[4,5], Brian Strahm[6] and Tyler Weiglein[6]*

[1] Department of Forest Engineering, Resources, and Management, Oregon State University, Corvallis, OR, United States, [2] Environmental Studies Program, Institute of Arctic and Alpine Research (INSTAAR), University of Colorado Boulder, Boulder, CO, United States, [3] USDA Forest Service, Northern Research Station, Houghton, MI, United States, [4] National Ecological Observatory Network, Boulder, CO, United States, [5] Institute of Arctic and Alpine Research (INSTAAR), University of Colorado Boulder, Boulder, CO, United States, [6] Department of Forest Resources and Environmental Conservation, Virginia Tech, Blacksburg, VA, United States

OPEN ACCESS

Edited by:
Evan S. Kane, Michigan Technological University, United States

Reviewed by:
José María De La Rosa, Institute of Natural Resources and Agrobiology of Seville (CSIC), Spain
José Manuel Moreno, University of Castilla La Mancha, Spain

***Correspondence:**
Jeff Hatten
jeff.hatten@oregonstate.edu

Specialty section:
This article was submitted to Fire and Forests, a section of the journal Frontiers in Forests and Global Change

Received: *25 October 2019*
Accepted: *14 January 2020*
Published: *04 February 2020*

Citation:
Matosziuk LM, Gallo A, Hatten J, Bladon KD, Ruud D, Bowman M, Egan J, Heckman K, SanClements M, Strahm B and Weiglein T (2020) Short-Term Effects of Recent Fire on the Production and Translocation of Pyrogenic Carbon in Great Smoky Mountains National Park. Front. For. Glob. Change 3:6. doi: 10.3389/ffgc.2020.00006

Fire affects the quantity and quality of soil organic matter (SOM). While combustion of the O-horizon causes direct losses of SOM, fire also transforms the remaining SOM into a spectrum of thermally altered organic matter. Pyrogenic carbon (PyC) can resist degradation and may have important effects on soil carbon cycling. The objectives of this study are to examine the mobility of PyC. Studying the effects of wildfire is challenging due to the rapid post-fire changes in the ecosystem and lack of robust controls. We overcame those limitations by examining the Chimney Tops 2 Fire which burned 4,617 ha of the Great Smoky Mountains National Park (GRSMNP), including a National Ecological Observatory Network (NEON) site, in November 2016. We examined PyC in soils from three time points from an area burned at low-severity (pre-, immediate post-, and 11 months post-fire) and two time points from areas burned at lower to higher severity (immediate post- and 11 months post-fire). At locations with pre-fire soil samples we found that PyC increased in the O-horizon (2.22 g BPCA/kg soil) after low severity fire, which resulted in higher PyC concentrations at 5–10 cm (0.73 g BPCA/kg soil and 17.79 g BPCA/kg C) and 10–20 cm (12.19 g BPCA/kg C) of depth in the mineral soil. Sites burned at higher severity had more PyC in the O horizon relative to sites burned at lower severity (10.29 g BPCA/kg soil and 29.89 g BPCA/kg C). As a result of higher concentrations of PyC in the O-horizons burned at higher severity, statistically more PyC moved from the O-horizon to the 0–10 cm horizon from immediate to 1-year post-fire (1.37 g BPCA/kg soil and 16.10 g BPCA/kg C). Lastly, the depth profile of C and BPCA suggest a shift in the source and amount of PyC in these soil profiles over time—possibly as a result of fire suppression. Results indicate that low severity fire may be an important mechanism by which PyC is produced and transported into mineral soils.

Keywords: pyrogenic carbon, NEON, fire, soil, carbon

INTRODUCTION

As the largest terrestrial carbon (C) reservoir, soils are a major component of the global carbon cycle (US Department of Energy Office of Science, 2009). Global fluxes of soil carbon occur on a massive scale, with microbial decomposition of soil organic matter (SOM) transferring ∼60 GT of carbon from soils to the atmosphere on an annual basis (US Department of Energy Office of Science, 2009). The balance between the carbon output of microbial decomposition and the carbon inputs from roots and above ground biomass determine whether soils act as either a carbon source or a carbon sink (Zomer et al., 2017). Consequently, due to the scale of C fluxes into and out of the soil, even a relatively small change in SOM decomposition rates can have a large impact on whether soils are a net sink or source of C to the atmosphere.

One of the largest unknowns in SOM research is the role of thermally-altered organic matter or pyrogenic carbon (PyC) in soil carbon storage (Preston and Schmidt, 2006; Schmidt et al., 2011; Santín et al., 2016). PyC is a broad term that refers to a spectrum of thermally altered organic matter formed through biomass burning or fossil fuel combustion (Schmidt and Noack, 2000; Preston and Schmidt, 2006; Singh et al., 2012; Bird et al., 2015). This spectrum of material, which encompasses a heterogeneous mixture of fire-altered residues that differ in physical size, formation temperature, chemical composition, resistance to degradation, and mechanism of formation (Masiello, 2004; Bird et al., 2015), plays a key role in soil carbon cycling. PyC is ubiquitous in both terrestrial and aquatic environments, making up an estimated 6% of the carbon in marine sediments (Masiello and Druffel, 1998), 10% of dissolved organic carbon fluxes to world oceans (Jaffé et al., 2013), and 14% of SOM (Reisser et al., 2016). Moreover, PyC is believed to decompose more slowly than unburned organic matter, with mean residence times on the order of multiple centuries rather than years or decades (Preston and Schmidt, 2006; Czimczik and Masiello, 2007; Bird et al., 2015). However, recent studies have suggested that PyC may cycle more rapidly under certain conditions depending on its physical and chemical interactions with the soil environment (Hockaday et al., 2006; Zimmermann et al., 2012; Lutfalla et al., 2017; De La Rosa et al., 2018). Given that the frequency and scale of wildfires are projected to continue to increase in the coming years due to the hotter, drier conditions associated with climate change (Dennison et al., 2014; Jolly et al., 2015; Abatzoglou and Williams, 2016), both the concentration of PyC on the landscape and the role that PyC plays in soil carbon cycling are also likely to increase. Thus, it is crucial that we develop a more complete understanding of the amount of PyC produced under different fire conditions as well as the movement of PyC and its interactions with the soil environment.

A great deal of research has been done to quantify and characterize the amount of PyC present in soil after a fire (Czimczik et al., 2005; Certini et al., 2011; Boot et al., 2015; Abney et al., 2017; Huang et al., 2018); however, there are several key gaps in the literature. Due to the unpredictable nature of fire, very few studies are able to make comparisons to pre-fire data (Abney et al., 2017; Doerr et al., 2018). Nearby unburned plots are typically used as references in such cases, but these plots may not be similar enough to draw comparisons, particularly in the case of low severity fire where it is unclear whether differences in pre-fire PyC concentrations have biased results (e.g., Czimczik et al., 2003; Boot et al., 2015). Additionally, only a few studies have compared the effects of low-severity and high-severity fire on soil PyC concentrations (Boot et al., 2015; Doerr et al., 2018; Huang et al., 2018). While a number of researchers have examined the effects of erosion on PyC movement (Rumpel et al., 2006; Cotrufo et al., 2016; Abney et al., 2017; Abney and Berhe, 2018) or the leaching of PyC from biochar (Major et al., 2010; Bostick et al., 2018), only a handful of studies (e.g., Abney et al., 2017) have performed repeated post-fire measurements to investigate the translocation of PyC from the forest floor to the mineral soil or the vertical movement of PyC through the soil profile.

In November 2016, the Chimney Tops 2 Fire burned over 4,617 ha of Great Smoky Mountains National Park (GSMNP) (National Park Service, US Department of the Interior Division of Fire and Aviation, 2017), including the National Ecological Observatory Network (NEON) site located near LeConte Creek (Thorpe et al., 2016). Prior to the fire, we had worked with NEON to collect several 50+ cm deep soil cores from the soil plots at the GSMNP site. This sampling effort provided a unique opportunity to leverage the pre-fire samples and collect information about the vertical movement of PyC following a wildfire. Thus, we resampled the area twice: 3 months post-fire and ∼1-year post-fire. The Chimney Tops 2 fire burned in a mosaic pattern, resulting in areas of high and low burn severity. All pre-fire samples were collected from soil plots burned under low severity. Post-fire samples were collected in these same soil plots and additional nearby plots that burned at low and high severity.

This unique data set allows us to overcome the challenges of comparing pre- and post-fire data and address several key questions regarding the production and movement of PyC under different burning conditions. (1) Does low-severity fire cause a detectable increase in soil PyC? (2) Is there a difference in either the quantity or chemical structure of PyC produced by high-severity and low-severity fire? (3) Does PyC migrate from the O-horizon to the mineral soil during the course of a 1-year period? In addition to these questions related to the Chimney Tops 2 fire, by sampling to a depth of 50 cm in a variety of landform positions, we were able to make inferences regarding the role of the historical fire regime in shaping the current distribution of PyC in GSMNP.

MATERIALS AND METHODS

Site and Fire Characteristics

The study sites are located within the Little River Ranger District of Great Smoky Mountains National Park, in the southern Appalachian Mountains of eastern Tennessee (35°41′20″N, 83°30′06″W). All plots were located between 570 and 805 m elevation, with slopes ranging from 0 to 30%. The plots are characterized as montane alluvial forest, submesic to mesic oak/hardwood forests, xeric pine woodland, southern Appalachian cove hardwood, and subxeric to xeric chestnut oak. Dominant tree species include eastern hemlock (*Tsuga*

canadensis (L.) Carrière), pitch pine (*Pinus rigida* Mill.), eastern white pine (*Pinus strobus* L.), hickory (*Carya sp.*), and red oak (*Quercus rubra* L.). The understory is dominated by mountain laurel (*Kalmia latifolia* L.) and rhododendron (*Rhododendron maximum* L.).

Soils are well-drained fine loams and coarse loams derived from metasedimentary sandstone and siltstone (Soil Survey Staff et al., 2019). Inceptisols are the dominant soil order at the soil plots, though Ultisols are present in several of the distributed plots (TW-51, TW-47, TW-53, TW-55, and TW-56). The top 50 cm of soil typically contains one to two A horizons (each 10–30 cm thick) above a Bw horizon that extends an additional 20–40 cm.

Climate data were retrieved from PRISM Data Explorer (http://www.prism.oregonstate.edu). Mean summer temperature at the NEON GRSMNP site (elev. 576 m) is 21°C and mean winter temperature is 2.4 °C. There is no distinct dry season in the region (monthly precipitation ranges from 85 to 146 mm), and mean annual precipitation at the site is 1,471 mm.

Fire history data suggests that prior to European settlement in the early to mid 1700s, the mean fire return interval in the area was ∼6–12 years (LaForest, 2012). Between 1834 and 1934, logging activity, and thus fire activity, increased dramatically. During that time, harvesting removed nearly 2/3 of forest cover and the mean fire return interval fell to 1.7–2.3 years.

The Chimney Tops 2 Fire was the largest fire in the history of the state of Tennessee, burning 4,617 ha in GSMNP. The fire was began November 23, 2016 as a result of human-caused ignition. The fire remained a small, low severity fire until November 27, 2016 when high winds caused the fire to spread rapidly. In addition to winds, the high rate of fire spread was due to a combination of drought, and seasonally dry fuels. Burn severity mapping found that 51.7 % was low-severity, 34.2 % was moderate-severity, 5.9 % was high-severity, while 7.4 % of the area within the fire perimeter was left unburned (**Figure 1**). Due to the low severity of this fire, field observed evidence of erosion was minimal during our field visits.

Sample Collection, Processing, and Characterization

Soil samples were collected from two different types of plots initially established by NEON: soil array plots and distributed plots. Soil array plots refer to the five plots in the NEON soil array (SP01-SP05) immediately surrounding the flux tower that experienced only low-severity fire during the Chimney Tops 2 fire (**Figure 2**). Distributed plots were also established by NEON and

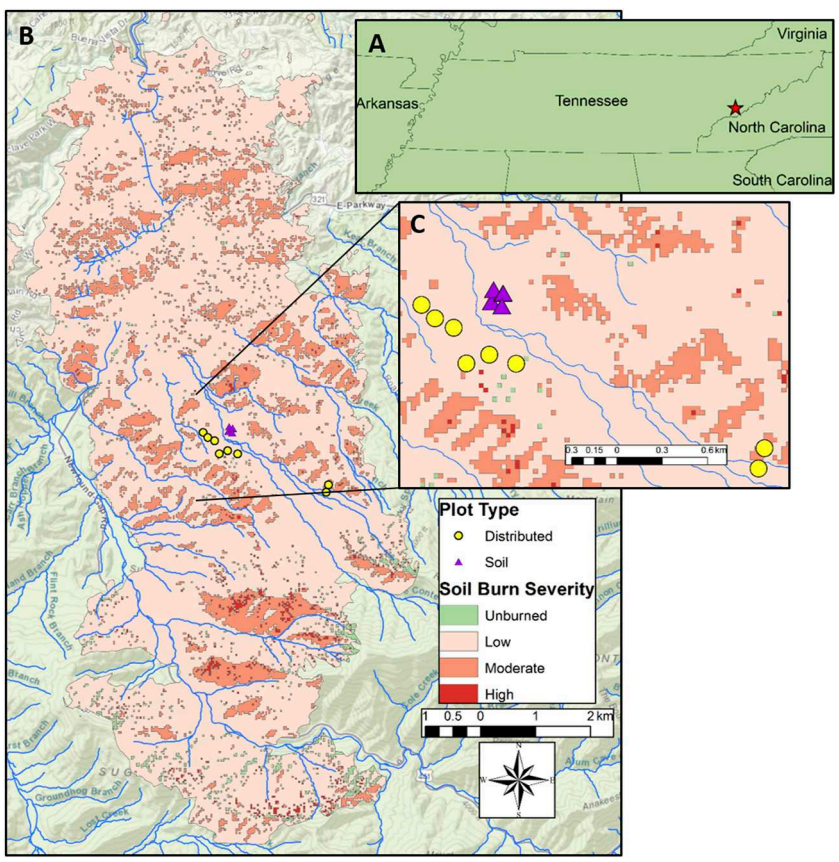

FIGURE 1 | (A) The study area is located in Great Smoky Mountains National Park in the Appalachian Mountains near the North Carolina-Tennessee border. **(B)** Soil burn severity map of the Chimney Tops 2 fire. **(C)** Soil array plots (purple triangles) are all located within low-severity areas while distributed plots (yellow circles) are located in areas with a broader range of burn severity.

FIGURE 2 | (Left) Example of low severity fire from the soil array (SP-01). Note the burned and unburned areas. **(Right)** Example of high severity fire from distributed plots (HI-01). This plot had >80% tree mortality and near complete combustion of O-horizon. Needle fall from fire-killed conifers covers the soil surface.

are dispersed over a wider spatial area and experienced a broader range of burn severity. Six of these distributed plots are NEON Tower Plots (unburned: TW-50; low-severity: TW-53, TW-55; moderate-severity: TW-47, TW-51, TW-56) located within the airshed boundary of the flux tower; DS-08 (unburned) is a NEON distributed plot located outside the airshed boundary; and HI-01 (high-severity) is a plot established specifically for this study that experienced high-severity fire. We attempted to limit our sampling to NEON maintained sample points in order to be able to leverage future work by NEON at these points.

Two different types of soil samples were analyzed in this study: core samples and grab samples. A pair of core samples was collected from each of the five soil array plots at each of three time points: pre-fire (August 2016), immediately post-fire (February 2017), and 1-year post-fire (November 2017). We collected soil cores (3.45 cm interior diameter) down to 50 cm in plastic liners that were housed within a gas-powered, stainless steel corer (9100 series Power Probe, AMS Inc.). Intact cores were capped, kept in a cooler, and shipped to the Oregon State University Marine Geological Repository Laboratory (MGRL), where they were stored at 4 °C until processing. Cores from the pre-fire and immediate post-fire time points were collected by the NEON team, while cores from the 1-year post-fire time point were collected by the authors. At the MGRL, one core of each pair ($n = 15$) was cut open, photographed, and described. Each core was divided into depth increments (0–5 cm, 5–10 cm, 10–20 cm, 20–30 cm, 30–50 cm), sieved to <2 mm while field moist, air-dried at room temperature, and ground to a fine powder using a roller grinder (SampleTek, model 200 vial rotator).

Grab samples were collected from distributed plots (8) at two different time points: immediately post-fire, and 1-year post-fire. For all grab samples a 30-cm deep pit was excavated just outside of each plot. The pit face was briefly described in our field notes, and grab samples collected at three depth increments: 0–10 cm, 10–20 cm, 20–30 cm using a stainless-steel trowel. Soils were air dried, sieved to <2 mm, and ground to a fine powder using a roller grinder.

O-horizon samples were collected from all soil array plots (5) at all three time points: pre-fire, immediately post-fire, and 1-year post-fire. O-horizon samples from the distributed plots (8) were only collected at the immediate post-fire and 1-year post-fire time points. O-horizon samples were oven-dried at 50°C until they reached a constant weight, subsampled, and ground to a fine powder using an IKA M20 Universal Mill.

Total carbon and nitrogen concentration of all soil samples was determined by combustion (Thermo FlashEA 1112 series, NC Soil Analyzer). Soil pH was determined using a 2:1 (w/w) mixture of water/soil (Thomas, 1996).

PyC Quantification and Characterization

The benzene polycarboxylic acid (BPCA) procedure originally developed by Glaser et al. (1998) takes a molecular marker approach to quantify and characterize PyC. Samples are digested in concentrated acid at elevated temperatures, oxidizing the carbon-carbon double bonds of the fused aromatic ring structures that form the molecular backbone of PyC. These aromatic structures are broken down into individual benzene rings substituted with carboxylic acids (i.e., benzene polycarboxylic acids or BPCAs; Glaser et al., 1998; Brodowski et al., 2005; Dittmar, 2008; Wiedemeier et al., 2013), which can be separated and quantified using high performance liquid chromatography (HPLC, **Supplementary Figure 1**) (Dittmar, 2008; Schneider et al., 2011; Wiedemeier et al., 2013).

PyC was quantified using the benzene polycarboxylic acid (BPCA) method, which uses nitric acid to oxidize the extended aromatic sheets characteristic of PyC into individual carboxylated benzene rings that can be isolated and quantified using high performance liquid chromatography (Glaser et al., 1998; Brodowski et al., 2005; Dittmar, 2008; Wiedemeier et al., 2013). Briefly, ground soil samples containing ∼2 mg of carbon were

digested in 5 mL HNO_3 at 170°C for 8 h using pressurized microwave vessels (Mars 6, CEM). Samples were filtered through glass fiber filters (Whatman, GF/A) and the remaining solids were washed with 5 mL of NaOH (1 M). Samples were diluted to 50 mL with deionized water, flash frozen with liquid nitrogen, and freeze dried (LabConco FreeZone Plus). The remaining residue was dissolved in 2 mL NaOH (1 M) and filtered using 0.45 μm nylon syringe filters (Whatman). A 1 mL aliquot of sample was transferred to a clean vial, spiked with 600 μL of HCl (2 M), and analyzed by HPLC (Shimadzu LC-10AD equipped with an SPD-M20A photodiode array capable of measuring wavelengths between 190 and 400 nm). An Agilent Poroshell 120 SB-C18 column was used with a mobile phase consisting of a binary gradient of H_3PO_4 (2% in water) and acetonitrile (Wiedemeier et al., 2013). External standards of pure BPCA solutions were used to construct 6-point calibration curves to determine the concentrations of individual BPCAs. Several tests with PyC-containing standard soils were performed to evaluate the reproducibility and accuracy of the method and are discussed in Matosziuk et al. (2019). By limiting our sample mass to <5 mg of carbon per digest we limit the error caused by the formation of BPCAs with three and four carboxyl groups that may be formed when digesting large amounts (>5 mg carbon) of organic rich matrices such as O-horizon (Kappenberg et al., 2016).

Many commonly used methods only quantify PyC (e.g., optical, thermal, and chemical methods), while the BPCA method provides additional information about the molecular structure of PyC (Hammes et al., 2007). When individual benzene rings are cleaved from the larger aromatic structure, the oxidation of each carbon-carbon bond typically creates a carboxylic acid substitution on the resulting benzene ring (Glaser et al., 1998). Thus, the carboxylic acid substitution pattern on individual BPCAs can theoretically reflect the relative position the ring held in the original aromatic structure. Rings near the edge of the aromatic structure can be cleaved by oxidizing only two or three carbon-carbon double bonds, resulting in BPCAs with few carboxylic acid substitutions (B2CAs and B3CAs). In contrast, the cleavage of internal rings requires the oxidation of six carbon-carbon bonds, producing BPCAs with six carboxylic acid substitutions (B6CAs). Thus, the B6CA:total BPCA ratio can theoretically serve as an aromatic condensation index (ACI)—because larger, more extended aromatic structures contain more interior benzene rings, a higher B6CA:total BPCA ratio (or higher ACI) reflects a greater degree of aromatic condensation (Schneider et al., 2010, 2011; 2013). Digestion of known precursors to test the correlation of molecular structure and BPCA products has rarely been done, but when conducted BPCA analysis of specific polyaromatic hydrocarbons (PAHs) has shown that ring substitution patterns do not necessarily correlate to PAH structure in a systematic way. However, in general, digestion of larger PAHs does result in more highly substituted BPCAs (Ziolkowski et al., 2011).

Statistical Methods

Individual samples from soil array and distributed plots were analyzed using separate statistical approaches. In both cases, multiple response variables were collected and analyzed, including the C and N concentration, C:N ratio, pH, and the quantity and chemical structure of PyC, which will be referred to as PyC concentration (g BPCA/kg C) and aromatic condensation index (ACI; g B6CA/g total BPCA), respectively. To ascertain whether PyC was translocated from the O-horizon to the mineral soil we calculated a ratio of the soil normalized PyC in the O-horizon to that in the surface mineral soil horizon (0–10cm) for the immediate post-fire and 1-year post-fire time points. As PyC was translocated from the O-horizon into the mineral soil the ratio will decrease. Each response variable for each depth increment was analyzed independently using R version 3.2.2. The significance level was set at alpha = 0.1.

Core Samples From Soil Array Plots

For each response variable at each depth, four linear mixed effects models were constructed where time since fire was the only fixed effect, plot was a random effect, and one of four possible correlation structures [no correlation, AR(1), compound symmetry, general correlation] was included to account for the temporal correlation. The anova function in R was used to compare the Bayesian information criterion (BIC) values for models with different correlation structures. For every response variable, at every depth, the simple model with no correlation structure was associated with the lowest BIC value or was within 2 units of the lowest BIC value. Consequently, for all subsequent temporal analysis of the cores, we used the simple model with no temporal correlation structure. Differences in time point were calculated using the EMmeans package in R (Lenth, 2016). Tukey corrections for family-wise error rates associated with pairwise comparisons of the 3 groups (pre-fire, immediate post-fire, and 1-year post-fire) were applied for all statistical tests on a given response variable.

Grab Samples From Distributed Plots

We utilized plots that had been established and will be monitored by NEON. The distributed plots burned at severities out of our control. To determine if either burn severity or time since fire affected response variables and have enough samples for statistical analysis, samples from the distributed plots were broadly characterized as "lower severity" or "higher severity" sites. Lower severity sites included plots classified as either "low-severity" ($n = 2$) or "unburned" ($n = 2$); higher severity sites included those that were classified as either "moderate" ($n = 3$) or "high-severity" ($n = 1$). Combining low-severity burn with unburned plots is not likely to confound our results as a result of the effects of low-severity wildfire being difficult to detect (e.g., Hatten et al., 2005) and we were unsure if the plots classified as unburned were actually unburned (we found no evidence of burning). While there may be different effects between moderate- and high-severity burns, we were only able to sample one plot burned at high-severity which we was combined with the plots burned at moderate-severity to balance the number of samples in the lower- and higher-severity classes ($n = 4$ each).

Burn severity at each plot was determined using field observations of char heights on trees, vegetation mortality, and O-horizon consumption. Burn severity was classified as

unburned, low, moderate, or high using a method adapted from Key and Benson (2006) by examining char height on trees, tree mortality, organic matter consumption, and presence of char (Hatten et al., 2008, 2012). A low-severity fire produced char heights <2 m on a tree bole and consumed little of the O horizon. Moderate-severity fires produced char heights between 2 and 4 m and left a thin layer of char on the surface of the soil. High-severity fire was designated when tree mortality was high and little O horizon remained. Plots where no evidence of burning was found were classified as unburned. For each response variable, at each depth, a linear mixed effects model was constructed where time since fire and burn severity were treated as fixed effects, and plot was included as a random effect. An overall F-test confirmed that for several response variables there was a significant interactive effect between burn severity and time since fire. Consequently, responses were analyzed to determine the conditional main effects of time since fire and burn severity. Multivariate t (MVT) corrections for multiple comparisons for family-wise error associated with four comparisons (low-severity vs. high-severity at both immediate post-fire and 1-year post-fire time points, and immediate post-fire vs. 1-year post-fire at both high and low-severity plots) were applied to all statistical tests.

RESULTS

Soil Array: Low-Severity

We detected very few statistically significant differences in soil properties between the three different time points at any given depth, likely due to the low burn severity at these plots (**Figure 3**). The concentration of PyC in the O-horizon was 2.22 g BPCA/kg soil higher in the immediate post-fire samples than in the pre-fire samples ($p = 0.07$), but not statistically different from the 1-year post-fire samples ($p = 0.35$) (**Table 1**). The 1-year post-fire samples have a greater concentration of PyC than the immediate post-fire samples at the 5–10 cm and 10–20 cm depths ($p = 0.09$ for both depths). The ACI of the immediate post-fire and 1-year post fire samples is 0.02 units lower than that of the pre-fire samples in the 0–5 cm depth ($p = 0.06$ for both time points), suggesting that the average structure of the PyC in the top 5 cm of mineral soil was less condensed following the fire. Compared to pre-fire samples, the pH of the 0–5 cm depth was 0.35 and 0.44 units lower at the immediate post-fire and 1-year post-fire time points ($p = 0.05$ and 0.02, respectively).

Distributed Plots: Low to High Severity

We detected an interactive effect between time since fire and burn severity for several response variables (**Table 2**). Consequently, the results are discussed as the conditional main effects of the two explanatory variables.

Effect of Burn Severity on SOM and PyC

At both post-fire time points, the mean O-horizon PyC concentration of the higher-severity plots was greater than that of the lower-severity plots (**Figure 4**); however, the magnitude of the difference was much greater at the immediate post-fire time point (29.89 g BPCA/kg C, $p = 0.001$) than at the 1-year post-fire time point (15.05 g BPCA/kg C, $p = 0.076$). At the 1-year post-fire time point, the mean 0-10 cm PyC concentration was 16.1 g BPCA/kg C greater in the higher-severity plots ($p = 0.051$); however, no differences in PyC between the burn severity sites were detected at this depth in the immediate post-fire samples. At depths below 10 cm we did not detect any differences in mean PyC concentration between higher- and lower-severity plots. While the O-horizon ACI was 0.11 units greater in the higher-severity plots at the immediate post-fire time point ($p = 0.034$), no differences in PyC structure were detected at any other depth or time point when comparing higher- and lower-severity plots.

At the 1-year post-fire time point, the mean 0–10 cm C and N concentrations were 1.54 and 0.24% greater in the lower-severity plots than the higher-severity plots, respectively ($p = 0.057$ and 0.081). At the immediate post-fire and 1-year post-fire time points, the mean 10–20 cm N concentrations were 0.13 and 0.15% greater in the lower-severity plots, respectively ($p = 0.005$ and 0.001). At the immediate post-fire time point, the mean C:N ratio of the lower-severity plots was lower than that of the higher-severity plots for all mineral soils (0–10, 10–20, and 20–30 cm), though this difference decreased with depth [13.71 ($p < 0.001$), 10.60 ($p = 0.009$), and 4.98 units ($p = 0.098$), respectively]. The effect of burn severity on C:N ratio was also significant in the 1-year post-fire samples; the mean 0–10 cm and 10–20 cm C:N ratios of the lower-severity plots were 20.32 and 9.41 units lower than the high severity plots, respectively ($p < 0.001$ and $p = 0.02$).

With the exception of the 0–10 cm depth at the immediate post-fire time point, the pH of the mineral soils was higher in the lower-severity plots than the higher severity plots at all depths at both time points. At the immediate post-fire time point, the differences in pH between the lower-severity and higher severity plots were 0.41 and 0.44 units at the 10–20 cm and 20–30 cm depths, respectively (p = 0.095 and 0.027). At the 1-year post-fire time point, the mean pH values of the lower-severity plots were 0.98 ($p = 0.063$), 0.49 ($p = 0.042$), and 0.49 ($p = 0.014$) units higher than the higher-severity plots for the 0–10, 10–20, and 20–30 cm depths, respectively.

Effect of Time Since Fire on SOM and PyC

The effect of time since fire on mean PyC quantity was only detectable in the higher-severity plots. In these plots, the mean O-horizon PyC concentration was 16.08 g BPCA/kg C (p = 0.084) and 6.32 g BPCA/kg soil ($p = 0.055$) greater immediately post-fire compared to 1-year post-fire. In contrast, the 0-10 cm PyC concentration was 1.38 g BPCA/kg soil greater at the 1-year post-fire time point ($p = 0.021$).

The effect of time since fire on PyC structure was only detectable in the O-horizon of lower-severity plots, where the ACI was 0.05 units <1-year post-fire. In the higher-severity plots, the mean 0–10 cm C:N ratio was 6.16 units <1-year post-fire compared to immediately post-fire ($p = 0.001$), while the mean 20–30 cm C:N ratio was 4.24 units greater than at the immediate post-fire time point ($p = 0.091$). We did not detect an effect of time since fire for any other response variables.

The ratio of PyC in the O-horizon to PyC in the mineral soil ($PyC_{OH/0-10}$) at both the immediate post-fire and 1-year post-fire time point illustrates translocation of PyC from the O-horizon into the mineral soil at (**Figure 5**). We found a

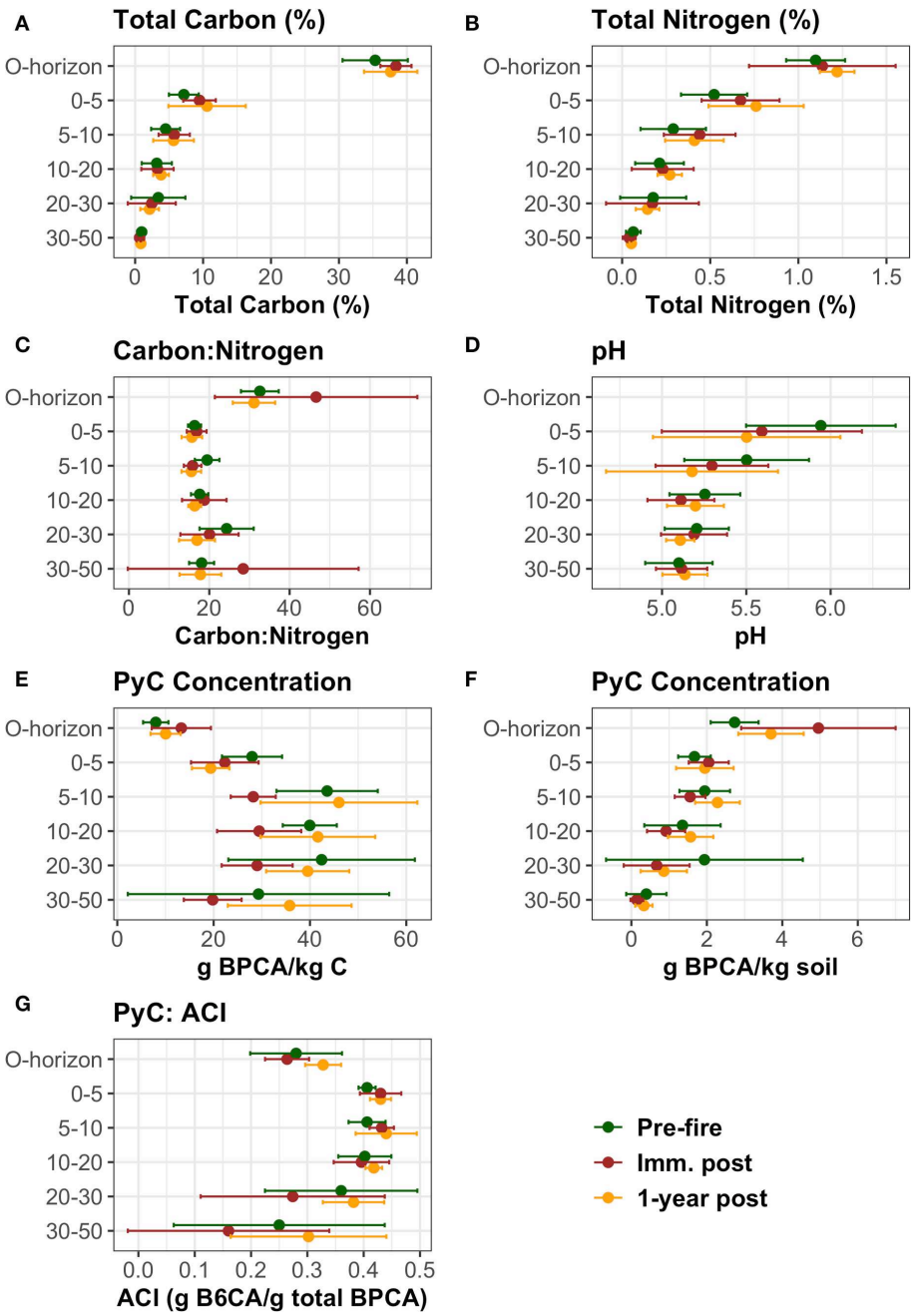

FIGURE 3 | (A) Total carbon, **(B)** total nitrogen, **(C)** C:N, **(D)** pH, **(E)** PyC concentration normalized by total carbon, **(F)** PyC concentration normalized by soil mass, and **(G)** ACI for core samples collected from the soil array that burned with low severity during the Chimney Tops 2 Fire. Circles denote mean values, error bars denote standard deviations.

significant interaction between time since fire and burn severity ($p = 0.0058$). The ratio of PyC in the O-horizon and mineral soil was greater in the higher-severity plots than lower-severity plots immediately post fire ($p = 0.0074$). However, 1-year post-fire there was no difference between the ratios of PyC in the O-horizon and mineral soils of lower- and higher-severity plots ($p > 0.1$). These results suggest that PyC has moved from the O-horizon into the mineral soil.

DISCUSSION

Effects of the Chimney Tops 2 Fire on SOM and Soil PyC

Low Severity Fire had Limited Effects on SOM and Soil PyC

Fire has complex effects on soil C and N concentrations, resulting from a variety of drivers that can have opposing effects dictated

TABLE 1 | Differences in response variables at different time points for core samples collected from the soil array plots that burned at low severity during the Chimney Tops 2 fire.

		Pre–fire– Imm. Post	Pre–fire – 1 year Post	Imm. Post– 1 year post
g BPCA/kg C	0–horizon	−5.3 ($p = 0.18$)	−2.04 ($p = 0.74$)	3.26 ($p = 0.48$)
	0–5 cm	5.65 ($p = 0.33$)	8.59 ($p = 0.11$)	2.94 ($p = 0.72$)
	5–10 cm	15.34 ($p = 0.15$)	−2.45 ($p = 0.94$)	**−17.79 ($p = 0.09$)**
	10–20 cm	10.51($p = 0.15$)	−1.68 ($p = 0.94$)	**−12.19 ($p = 0.09$)**
	20–30 cm	13.39 ($p = 0.29$)	2.89 ($p = 0.93$)	−10.5 ($p = 0.44$)
	30–50 cm	10.66 ($p = 0.57$)	−5.32 ($p = 0.86$)	−15.99 ($p = 0.22$)
g BPCA / kg soil	0–horizon	**−2.22 ($p = 0.07$)**	−0.96 ($p = 0.52$)	1.26 ($p = 0.35$)
	0–5 cm	−0.38 ($p = 0.49$)	−0.28 ($p = 0.67$)	0.1($p = 0.94$)
	5–10 cm	0.39 ($p = 0.42$)	−0.34 ($p = 0.51$)	**−0.73 ($p = 0.09$)**
	10–20 cm	0.43 ($p = 0.61$)	−0.22 ($p = 0.88$)	−0.65 ($p = 0.35$)
	20–30 cm	1.27 ($p = 0.25$)	1.08 ($p = 0.35$)	−0.19 ($p = 0.96$)
	30–50 cm	0.29 ($p = 0.28$)	0.11($p = 0.81$)	−0.18 ($p = 0.46$)
ACI	0–horizon	0.02 ($p = 0.89$)	−0.05 ($p = 0.39$)	−0.06 ($p = 0.21$)
	0–5 cm	**−0.02 ($p = 0.06$)**	**−0.02 ($p = 0.06$)**	0 ($p = 1$)
	5–10 cm	−0.03 ($p = 0.56$)	−0.03 ($p = 0.39$)	−0.01($p = 0.94$)
	10–20 cm	0.01($p = 0.97$)	−0.02 ($p = 0.81$)	−0.02 ($p = 0.67$)
	20–30 cm	0.09 ($p = 0.54$)	−0.02 ($p = 0.96$)	−0.11 ($p = 0.39$)
	30–50 cm	0.15 ($p = 0.32$)	0 ($p = 1$)	−0.14 ($p = 0.23$)
C%	0–horizon	−3.06 ($p = 0.45$)	−2.28 ($p = 0.63$)	0.77 ($p = 0.95$)
	0–5 cm	−2.3 ($p = 0.62$)	−3.42 ($p = 0.37$)	−1.11 ($p = 0.89$)
	5–10 cm	−1.27 ($p = 0.58$)	−1.17 ($p = 0.63$)	0.1($p = 1$)
	10–20 cm	−0.1($p = 0.99$)	−0.62 ($p = 0.78$)	−0.52 ($p = 0.84$)
	20–30 cm	0.95 ($p = 0.64$)	1.28 ($p = 0.47$)	0.32 ($p = 0.95$)
	30–50 cm	0.42 ($p = 0.45$)	0.25 ($p = 0.74$)	−0.17 ($p = 0.81$)
N%	0–horizon	−0.04 ($p = 0.97$)	−0.12 ($p = 0.75$)	−0.08 ($p = 0.87$)
	0–5 cm	−0.15 ($p = 0.56$)	−0.24 ($p = 0.26$)	−0.09 ($p = 0.81$)
	5–10 cm	−0.15 ($p = 0.32$)	−0.12 ($p = 0.46$)	0.03 ($p = 0.95$)
	10–20 cm	−0.02 ($p = 0.96$)	−0.06 ($p = 0.7$)	−0.04 ($p = 0.84$)
	20–30 cm	0 ($p = 1$)	0.03 ($p = 0.9$)	0.03 ($p = 0.92$)
	30–50 cm	0.02 ($p = 0.58$)	0.01($p = 0.87$)	−0.01($p = 0.81$)
C:N	0–horizon	−14 ($p = 0.28$)	1.46 ($p = 0.98$)	15.46 ($p = 0.23$)
	0–5 cm	−0.53 ($p = 0.91$)	0.67 ($p = 0.86$)	1.19 ($p = 0.63$)
	5–10 cm	3.61($p = 0.1$)	3.93 ($p = 0.07$)	0.32 ($p = 0.98$)
	10–20 cm	−1.14 ($p = 0.87$)	1.23 ($p = 0.85$)	2.37 ($p = 0.57$)
	20–30 cm	4.26 ($p = 0.55$)	7.36 ($p = 0.21$)	3.1($p = 0.72$)
	30–50 cm	−10.54 ($p = 0.72$)	0.12 ($p = 1$)	10.65 ($p = 0.64$)
pH	0–5 cm	**0.35 ($p = 0.05$)**	**0.44 ($p = 0.02$)**	0.09 ($p = 0.76$)
	5–10 cm	0.21($p = 0.42$)	0.32 ($p = 0.15$)	0.12 ($p = 0.73$)
	10–20 cm	0.14 ($p = 0.48$)	0.06 ($p = 0.89$)	−0.09 ($p = 0.75$)
	20–30 cm	0.02 ($p = 0.98$)	0.1($p = 0.58$)	0.08 ($p = 0.68$)
	30–50 cm	0 ($p = 1$)	−0.02 ($p = 0.96$)	−0.02 ($p = 0.96$)

Differences calculated using the CMmeans package in R (Lenth, 2016). Bold indicates statistical significance.

by burn severity (Nave et al., 2011; Pellegrini et al., 2017). The Chimney Tops 2 Fire burned in a mosaic pattern and distinct regions within the burn perimeter experienced moderate- to high-severity fire, but the majority of the landscape burned at low severity (**Figure 1**). Using core samples collected from the soil array plots that experienced only low severity fire, we did not detect any differences between pre-fire and either immediate post-fire or 1-year post-fire concentrations of C or N, suggesting that this fire did not alter SOM concentrations near the NEON flux tower. Because these plots were clustered in a single alluvial plain near LeConte Creek, we cannot extrapolate our results to all low-severity areas within the burn perimeter. However, it is likely that the Chimney Tops 2 Fire did not alter short-term C or N concentrations in regions located at

TABLE 2 | Differences in mean response variables at different time points for grab samples collected at the distributed plots from both immediately post-fire and 1-year post-fire from soil plots that burned at lower and higher severity during the Chimney Tops 2 fire.

		(Lower Severity– Higher Severity)		(1 year post fire– Imm.Post Fire)		Interactive Effect
		Imm.Post–fire	1–year Post–fire	Higher Severity	Lower Severity	Severity x Time p–val
gPyC/kgC	0–horizon	**−29.89 ($p = 0.001$)**	**−15.05 ($p = 0.076$)**	**−16.08 ($p = 0.084$)**	−1.24 ($p = 0.988$)	**0.075**
	0–10 cm	−6.12 ($p = 0.661$)	−16.1($p = 0.051$)	9.23 ($p = 0.395$)	−0.75 ($p = 0.997$)	0.192
	10–20 cm	−3.32 ($p = 0.911$)	−6.01($p = 0.649$)	2.18 ($p = 0.958$)	−0.52 ($p = 0.998$)	0.643
	20–30 cm	−4.21($p = 0.946$)	12.01($p = 0.449$)	−8.98 ($p = 0.642$)	7.24 ($p = 0.501$)	0.12
g PyC / kg soil	0–horizon	**−10.29 ($p = 0.007$)**	−4.74 ($p = 0.258$)	**−6.32 ($p = 0.055$)**	−0.76 (p−0.945)	0.063
	0–10 cm	0.14 ($p = 0.983$)	**−1.37 ($p = 0.024$)**	**1.38 ($p = 0.021$)**	−0.13 ($p = 0.954$)	**0.011**
	10–20 cm	0.13 ($p = 0.951$)	0.42 ($p = 0.387$)	−0.23 ($p = 0.695$)	0.06 ($p = 0.965$)	0.294
	20–30 cm	0.45 ($p = 0.622$)	0.76 ($p = 0.23$)	−0.24 ($p = 0.94$)	0.07 ($p = 0.995$)	0.591
ACI	0–horizon	**−0.11($p = 0.034$)**	−0.02 ($p = 0.896$)	−0.04 ($p = 0.439$)	**0.05 ($p = 0.068$)**	**0.02**
	0–10 cm	0.06 ($p = 0.427$)	0.06 ($p = 0.433$)	−0.03 ($p = 0.912$)	−0.03 ($p = 0.752$)	0.991
	10–20 cm	0.03 ($p = 0.832$)	0.03 ($p = 0.671$)	−0.0l ($p = 0.974$)	0 ($p = 0.998$)	0.816
	20–30 cm	0.09 ($p = 0.789$)	0.13 ($p = 0.519$)	−0.05 ($p = 0.959$)	0 ($p = 1$)	0.712
C{%)	0–horizon	0.77 (p−0.999)	0.5 ($p = 1$)	−3.71(p−0.919)	−3.98 (p−0.745)	0.973
	0–10 cm	−0.13 ($p = 1$)	−0.34 ($p = 0.995$)	0.34 ($p = 0.996$)	0.13 ($p = 0.999$)	0.921
	10–20 cm	0.63 ($p = 0.621$)	**1.54 ($p = 0.057$)**	−0.73 ($p = 0.621$)	0.18 ($p = 0.965$)	0.259
	20–30 cm	2.12 ($p = 0.188$)	1.19 ($p = 0.616$)	−0.51($p = 0.967$)	−1.44 ($p = 0.284$)	0.535
N(%)	0–horizon	0.25 ($p = 0.484$)	0.28 ($p = 0.385$)	−0.01($p = 1$)	0.02 ($p = 0.994$)	0.841
	0–10 cm	0.2 ($p = 0.158$)	**0.24 ($p = 0.081$)**	−0.03 ($p = 0.992$)	0.01($p = 0.997$)	0.755
	10–20 cm	**0.13 ($p = 0.005$)**	**0.15 ($p = 0.001$)**	−0.02 ($p = 0.89$)	0 ($p = 1$)	0.633
	20–30 cm	0.17 ($p = 0.068$)	0.1($p = 0.409$)	−0.02 ($p = 0.994$)	−0.09 ($p = 0.261$)	0.427
C:N	0–horizon	−6.22 ($p = 0.91$)	−18.46 ($p = 0.273$)	−0.52 ($p = 1$)	−12.75 ($p = 0.209$)	0.309
	0–10 cm	**−13.71 ($p = 0$)**	**–20.32 ($p = 0$)**	**6.16 ($p = 0.001$)**	−0.45 ($p = 0.917$)	**0.001**
	10–20 cm	**−10.6 ($p = 0.009$)**	**−9.41($p = 0.02$)**	−0.03 ($p = 1$)	1.17 ($p = 0.842$)	0.671
	20–30 cm	**−4.98 ($p = 0.098$)**	−1.09 ($p = 0.936$)	**−4.24 ($p = 0.091$)**	−0.34 ($p = 0.987$)	0.08
pH	0–10 cm	0.62 ($p = 0.306$)	**0.98 ($p = 0.063$)**	0.09 ($p = 0.992$)	0.44 ($p = 0.209$)	0.392
	10–20 cm	**0.41($p = 0.095$)**	**0.49 ($p = 0.042$)**	0.07 ($p = 0.959$)	0.15 ($p = 0.469$)	0.695
	20–30 cm	**0.44 ($p = 0.027$)**	**0.49 ($p = 0.014$)**	0.04 ($p = 0.992$)	0.09 ($p = 0.782$)	0.79

Differences calculated using the EMmeans package in R (Lenth, 2016). Bold indicates statistical significance.

similar elevations and topographic positions that burned at low severity.

The BPCA method we used in this study characterized both PyC quantity and molecular structure. While the total concentration of BPCAs (g BPCA/kg C or g BPCA/kg soil) reflects the quantity of PyC in the soil, the relative proportion of the various BPCAs that were extracted (B*n*CA, for $n = 3$, 4, 5, or 6, where n is the number of carboxylic acid substitutions on an individual benzene ring) reflect its molecular structure. A greater proportion of B6CA, referred to here as ACI, indicates PyC with a more extended aromatic structure. Such structures are associated with both higher pyrolysis temperatures (McBeath et al., 2011; Schneider et al., 2013) and longer mean residence times in the soil (Baldock and Smernik, 2002; Singh et al., 2012; Bird et al., 2015; Gibson et al., 2018).

The concentration of PyC in samples collected from all plots in this study was quite high; on average, mineral soils down to 50 cm contained 25–40 g BPCA/kg C. The PyC concentration of the GSMNP samples was on par with or greater than published values from study areas that have historically experienced frequent fire and/or currently include prescribed burns as part of their management plan (Boot et al., 2015; Matosziuk et al., 2019; Soucémarianadin et al., 2019). This is consistent with the current conceptual model of historical fire frequency in the Southern Appalachian region, which proposes that frequent burning occurred in the area during all phases of land use, with the exception of the fire-exclusion era of the twentieth century (Harmon, 1982; Delcourt and Delcourt, 1997; Lafon et al., 2017).

The low severity fire at the soil array plots had a limited effect on PyC concentration. The O-horizon PyC concentration of the immediate post-fire samples was slightly higher than that of the pre-fire samples; however, this difference was not detectable 1 year later, likely due to the combined effects of lateral/vertical movement of PyC and dilution from fresh litterfall. At the 5–10 and 10–20 cm depths, the mean concentration of PyC in the 1-year post-fire samples was greater than that of the immediate post-fire samples. This could be due to vertical movement of PyC from the O-horizon into the mineral soil over the course of the year following the fire. However, this conclusion is questionable as there is no difference in PyC concentrations either between the pre-fire and 1-year post-fire samples at these same depths or between any of the time points at the 0–5 cm depth.

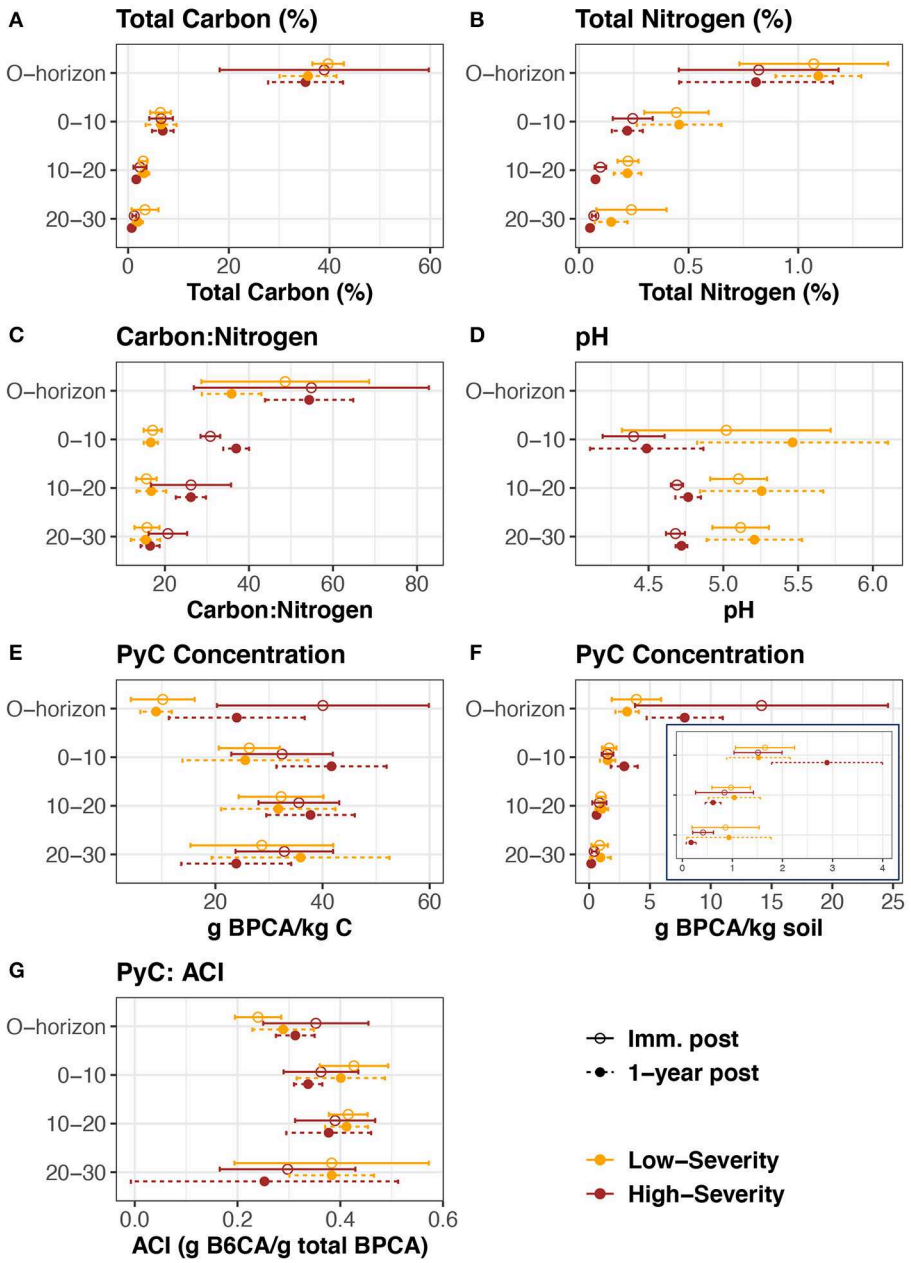

FIGURE 4 | (A) Total carbon, **(B)** total nitrogen, **(C)** C:N, **(D)** pH, **(E)** PyC concentration normalized by total carbon, **(F)** PyC concentration normalized by soil mass, and **(G)** ACI for grab samples collected from distributed plots that burned with lower severity and higher severity during the Chimney Tops 2 Fire. Inset in **(F)** of the PyC concentration of mineral soil horizons. Circles denote mean values, error bars denote standard deviations.

The molecular structure of PyC in the soil array plots, as determined by ACI was also relatively unchanged by the Chimney Tops 2 fire. The small (0.02 unit) post-fire increase in mean ACI of the 0–5 cm samples suggests that the PyC produced by the fire was slightly more condensed than the PyC already present in the soil; however, the magnitude of this difference was quite small. The mean 0–5 cm ACI for both the immediate post-fire and 1-year post-fire samples was 0.43, compared to 0.41 for the pre-fire samples. ACI is associated with both the formation temperature of char and its mean residence time in the soil. Higher pyrolysis temperatures typically produce more condensed PyC (i.e., PyC with a higher ACI) with longer MRTs as found by Gibson et al. (2018) found that mean residence time of PyC shifts from the decadal scale to the centennial scale at pyrolysis temperatures between 450 and 500°C. Additionally, Schneider et al. (2011) performed BPCA analysis on a thermosequence of chars pyrolyzed in a muffle furnace, as well as those burned at known temperature in an experimental forest fire (Schneider et al., 2013). According to these results, ACI values of both 0.43 and 0.41 likely correspond to chars that were formed at

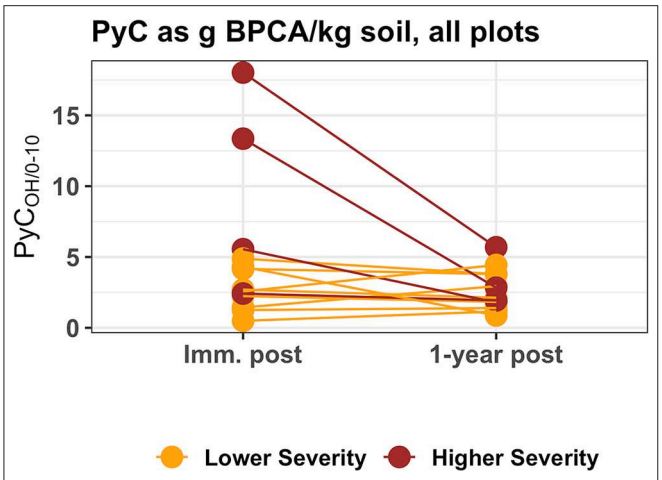

FIGURE 5 | A comparison of the soil mass normalized ratio of PyC in the O-horizon to PyC in the mineral soil ($PyC_{OH/0-10}$) at the immediate post-fire and 1-year post-fire time point.

temperatures above 500°C. Thus, the small post-fire increase in ACI is unlikely to have a meaningful effect on PyC turnover in these plots.

Moderate to High Severity Fire Results in Greater PyC Inputs to the O-Horizon, Which Begin Moving Into the Mineral Soil Within 1 Year of Fire

PyC concentration depended on both burn severity and time since fire, with trends differing at different depths. In the O-horizon, the high-severity plots had a greater mean concentration of PyC than the low-severity plots at both time points; however, the difference was more pronounced immediately post-fire compared to 1-year post-fire. In the 0–10 cm layer, the mean PyC concentration was greater in the higher-severity plots compared to the lower-severity plots, but in contrast to the trend in the O-horizon, this difference was only observed at the 1-year post-fire time point. Additionally, for the higher-severity sites, the O-horizon PyC concentration was higher at the immediate post-fire time point compared to the 1-year post-fire time point, while the 0–10 cm PyC concentration was greatest at the 1-year post fire time point.

These observations are consistent with a conceptual model based on the movement of PyC from the O-horizon to the mineral soil. The Chimney Tops 2 fire produced significant PyC input to the O-horizons of the higher-severity plots but not necessarily to the low-severity plots. Consequently, during the immediate post-fire time point we observed a large difference between the higher- and lower-severity plots in terms of O-horizon PyC concentrations. Over the course of the year, a portion of the PyC in the O-horizon of higher-severity plots moved vertically into the soil profile or horizontally due to leaching/erosion. This is consistent with a preliminary study on these sites, which found ∼1.8-times higher saturated hydraulic conductivity on the high burn severity areas compared to the low severity and unburned areas due to altered soil structure during the combustion process (**Supplementary Material**). Higher rates of water flux into and through the soils at the high burn severity sites may have increased the rate of movement of small particulate material or dissolved forms of char through the soil. Thus, not only was there more PyC in areas burned at high severity, but the potential for this material to be transported to depth in the soil may also have been higher. At the immediate post-fire time point, little of the PyC generated in the Chimney Tops 2 fire had been incorporated into the mineral soil. However, over the course of the year, a portion of the PyC introduced to the O-horizon in the higher-severity sites may have moved into the mineral soil. Thus, at the 1-year post-fire time point, the PyC concentration of the 0–10 cm depth was notably higher at the higher-severity sites compared to the lower-severity sites. This was illustrated by comparing the ratio of PyC in the O-horizon to PyC in the mineral soil ($PyC_{OH/0-10}$) at both the immediate post-fire and 1-year post-fire time point (**Figure 5**).

Several different mechanisms could contribute to the decrease in O-horizon PyC concentration in the year since the fire including vertical movement of PyC into the soil profile, loss of PyC from the site due to lateral movement (wind/water erosion), or dilution of PyC due to the deposition of new litterfall. To examine the relative contribution of vertical movement vs. erosion/dilution, we defined a new variable, $PyC_{1yr/imm,}$, as the ratio of the PyC concentration in a given depth at the 1-year post-fire time point to the concentration in the same depth at the immediate post-fire time point (**Figure 6**). This ratio is a measure of whether PyC concentration is increasing or decreasing over time in a given soil horizon; a ratio <1 indicates that the PyC concentration at that depth has decreased over the year, while a ratio >1 suggests the PyC concentration increased. If PyC is indeed moving vertically from the O-horizon into the mineral soil, we would expect to see many points in the upper left quadrant of this plot, which indicates a decrease in O-horizon PyC concentration and an increase in 0–10 cm PyC concentration over the course of the year. In contrast, if the reduction in O-horizon PyC over time is due to erosion or dilution, we would expect to see many points that are either in the lower left quadrant or on the left hand side of the plot near the midline at 1.0, which would indicate either a reduction of PyC at both depths or a reduction of PyC in the O-horizon with no change in 0–10 cm PyC concentration, respectively. Points on the upper and lower right quadrants of the plot, which correspond to a gain in PyC at both depths and a gain in O-horizon PyC and a loss of 0–10 cm PyC, respectively, suggest that there has been additional input of PyC since the fire. This may occur as charred bark or snags begin to decompose and deposit PyC onto the soil surface.

Most points lay in either the upper left-hand corner, or on the left side near the midline, suggesting that a combination of vertical movement and erosion/dilution are responsible for the reduction in O-horizon PyC concentration in the year after the fire. Erosion may alter mean residence time estimates by up to 150 years (Abney and Berhe, 2018), so we investigated whether the relative values of O-horizon and 0–10 cm $PyC_{1yr/imm}$ at a given plot were related to its potential for erosion based on slope and landform position, but did not find a clear pattern,

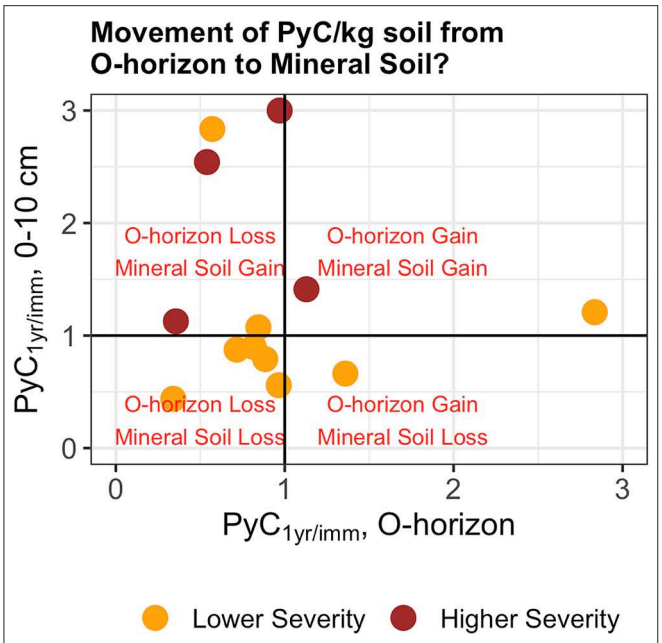

FIGURE 6 | The soil mass normalized ratio of PyC concentration in a given depth at the 1-year post-fire time point to the concentration in the same depth at the immediate post-fire time point ($PyC_{1yr/imm}$) is a measure of whether PyC concentration is increasing or decreasing over time; a ratio <1 indicates that the PyC concentration at that depth has decreased over the year, while a ratio >1 suggests the PyC concentration increased.

which may suggest that both dilution and erosion play a role. Unfortunately, O-horizon samples from this study were not collected volumetrically, so we could not determine the mass of PyC that was moved laterally due to erosion or vertically from the O-horizon to the mineral soil.

The fact that a detectable amount of PyC moves from the O-horizon into the mineral soil <1 year after fire has important implications for PyC cycling as this translocation may offer protection from both biotic and abiotic degradation. The two primary mechanisms that protect organic matter from microbial decomposition, association with a mineral surface or incorporation within soil aggregates, only affect organic matter that is in the mineral soil (Lehmann and Kleber, 2015). Moreover, the consumption of surface PyC in subsequent fires has been posited as a significant mechanism for abiotic PyC decomposition (Santín et al., 2013; Masiello et al., 2015; Doerr et al., 2018). Mineral soil has a tremendous capacity to act as a temperature buffer during fires (González-Pérez et al., 2004; Certini, 2005). Due to the protections offered by the mineral soil, the movement of PyC from the O-horizon into the soil profile on such a short time scale is likely to result in higher mean residence times than if the material remained on the forest floor for a more extended period of time.

Legacy Effects of Previous Fires

Translocation of PyC From the O-Horizon to the Mineral Soil Is Associated With an Increase in ACI

When averaged over all time points, the mean ACI of the PyC in the O-horizon of the core samples was 0.13 units lower than that of the 0–5 cm layer ($p < 0.0001$), suggesting that the PyC in the mineral soil is more condensed than that in the O-horizon. A similar trend exists for the grab samples—when averaged over all time points and all fire severities, the mean ACI of the O-horizon is 0.11 units lower than that of the 0–10 cm layer. This pattern of PyC condensation increasing with depth is consistent with the findings of Boot et al. (2015) who found that the proportion of B6CA extracted from 5 to 15 cm was statistically greater than that of the forest floor. Similarly, Soucémarianadin et al. (2019) found that the proportion of B3CA in mineral soils decreased with depth, and attributed their observation partly to oxidation of highly condensed PyC into heavily oxygenated, and thus more soluble components. Abiven et al. (2011) found that a significant amount of condensed PyC could be extracted from aged char that had been left exposed in the field, confirming that PyC can move vertically through the soil profile as dissolved organic matter.

Another possible explanation is that the physical characteristics of high temperature (and thus more condensed) PyC promote its incorporation into the mineral soil. PyC that is formed at higher temperatures bears less resemblance to the organic matter it originated from, leaving fewer structural components to hold the material together (Soucémarianadin et al., 2013). Consequently, it may be easier to fragment, which may facilitate its downward movement into the soil profile.

Regardless of the mechanism responsible, the fact that more condensed PyC is concentrated in the mineral soil compared to the O-horizon may partly explain the association between the degree of aromatic condensation and mean residence time. A number of studies have suggested that PyC with a more condensed chemical structure is more likely to resist decomposition (Baldock and Smernik, 2002; Singh et al., 2012; Bird et al., 2015; Gibson et al., 2018). However, it is possible that this increase in mean residence time comes in part from the fact that more condensed PyC can be more efficiently translocated from the forest floor to the mineral soil where it can be protected from biotic decomposition and abiotic degradation by either association with a mineral surface or incorporation into an aggregate (Brodowski et al., 2006; Heckman et al., 2014).

Changes in Fire Frequency May Alter the Vertical Distribution of PyC in Soil

The concentration of PyC at soil depths >15 cm are not frequently reported, but both Soucémarianadin et al. (2019) and Butnor et al. (2017) found that while PyC concentrations as a proportion of soil decreased with depth, the concentration as a proportion of soil carbon remained fairly constant. We found similar results in this study at depths below 10 cm; however, from 0–5 to 5–10 cm the mean concentration of PyC as a proportion of carbon increased from 29.2 to 39.3 g BPCA/kg C. If the concentration of PyC as a proportion of carbon was constant with depth, we would expect a strong correlation between carbon concentration (%C) and PyC concentration (g BPCA/kg C). In our data set there was indeed a strong correlation between the two ($R^2 = 0.8$), but only for samples taken below 10 cm. For samples taken from 0–5 to 5–10 cm, this correlation was much weaker ($R^2 = 0.29$) (**Figure 7**).

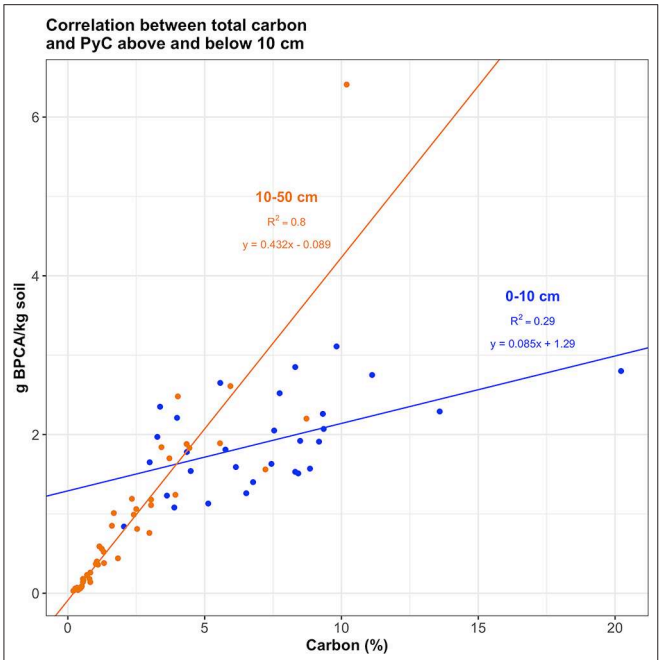

FIGURE 7 | There was a strong correlation ($R^2 = 0.80$) between carbon concentration and PyC concentration at depths below 10 cm (orange); however, this correlation is much weaker ($R^2 = 0.29$) in the top 10 cm (blue).

This may be a result of the changes in fire regime that have taken place in this region over the past few centuries. Until the early twentieth century, the mean fire return interval for this area ranged between 2 and 12 years (LaForest, 2012; Lafon et al., 2017). Thus, for centuries the soils of this area received regular inputs of PyC, which likely moved vertically through the soil profile at a rate similar to other organic matter. However, after the implementation of fire suppression PyC inputs were undoubtably reduced, while other organic inputs from litter and fine roots may have remained constant. As a result, the PyC concentration in the upper parts of the soil profile would have become diluted. Prescribed fire is becoming a more common tool for fuel reduction in some areas of the Southern Appalachians. It is possible that as fire is reintroduced to this landscape, and the PyC inputs to the soil become more regular, the correlation between carbon concentration and PyC concentration in the upper parts of the profile will strengthen.

CONCLUSIONS

Samples collected from Great Smoky Mountains National Park before and after the Chimney Tops 2 Fire have provided substantial insight into several open questions regarding PyC production and movement under different conditions. We found that low-severity fire slightly increased the PyC concentrations in the O-horizon, but the effect was so small it had no effect on mineral soil within 1 year of the fire. However; 3 months post-fire, sites that burned with mid- to high-severity had statistically higher PyC concentrations in the O-horizon compared with low-severity sites. In the year following the fire, at the higher-severity sites the PyC concentration of the O-horizon decreased while the concentration of the 0–10 cm depth increased, suggesting that movement of PyC from the O-horizon to the mineral soil begins <1-year post fire. This rapid incorporation into mineral soil where a variety of mechanisms can provide protection from biotic and abiotic degradation may play a role in the long residence time of PyC in soil. Lastly, while several earlier studies have found that PyC concentration as a proportion of carbon remains constant with depth, we only found a correlation between %C and PyC concentration at depths below 10 cm. This may reflect the reduction in PyC input that has occurred in recent years as a result of fire suppression.

DATA AVAILABILITY STATEMENT

All datasets generated for this study are included in the article/**Supplementary Material**.

AUTHOR CONTRIBUTIONS

JH, LM, KB, DR, KH, MS, and BS were involved with the conception and design of the study. LM, AG, JH, KB, DR, JE, and TW were involved with the acquisition, analysis and/or interpretation of data. LM, JH, KB, DR, MB, JE, KH, MS, BS, and TW were involved with the writing and revising of the manuscript.

FUNDING

This material was based upon work supported by the National Science Foundation under Grant Number NSF−1733885 and 1340504.

ACKNOWLEDGMENTS

We would like to thank the Great Smoky Mountain National Park staff for the support of this work which was authorized under permit number GRSM-2017-SCI-1296. We acknowledge the National Science Foundation for supporting the construction and ongoing operation of NEON. NEON is a project solely sponsored by the NSF and managed under cooperative support agreement (EF-1029808) to Battelle. We would like to thank Rommel Zulueta and the NEON SI Team for their support and assistance in the field for this project. Finally, we would like to acknowledge that the Chimney Tops 2 fire resulted in the deaths of fourteen people, and the destruction or damage of 2,500 homes and businesses.

SUPPLEMENTARY MATERIAL

The Supplementary Material for this article can be found online at: https://www.frontiersin.org/articles/10.3389/ffgc.2020.00006/full#supplementary-material

REFERENCES

Abatzoglou, J. T., and Williams, A. P. (2016). Impact of anthropogenic climate change on wildfire across western US forests. *Proc. Natl. Acad. Sci. U.S.A.* 113, 11770–11775. doi: 10.1073/pnas.1607171113

Abiven, S., Hengartner, P., Schneider, M. P. W., Singh, N., and Schmidt, M. W. I. (2011). Pyrogenic carbon soluble fraction is larger and more aromatic in aged charcoal than in fresh charcoal. *Soil. Biol. Biochem.* 43, 1615–1617. doi: 10.1016/j.soilbio.2011.03.027

Abney, R. B., and Berhe, A. A. (2018). Pyrogenic carbon erosion: implications for stock and persistence of pyrogenic carbon in soil. *Front. Earth Sci.* 6:26. doi: 10.3389/feart.2018.00026

Abney, R. B., Sanderman, J., Johnson, D., Fogel, M. L., and Berhe, A. A. (2017). Post-wildfire erosion in mountainous terrain leads to rapid and major redistribution of soil organic carbon. *Front. Earth Sci.* 5:99. doi: 10.3389/feart.2017.00099

Baldock, J. A., and Smernik, R. J. (2002). Chemical composition and bioavailability of thermally altered Pinus resinosa (Red pine) wood. *Org. Geochem.* 33, 1093–1109. doi: 10.1016/S0146-6380(02)00062-1

Bird, M. I., Wynn, J. G., Saiz, G., Wurster, C. M., and McBeath, A. (2015). The Pyrogenic Carbon Cycle. *Annu. Rev. Earth Planet. Sci.* 43, 273–298. doi: 10.1146/annurev-earth-060614-105038

Boot, C. M., Haddix, M., Paustian, K., and Cotrufo, M. F. (2015). Distribution of black carbon in ponderosa pine forest floor and soils following the High Park wildfire. *Biogeosciences* 12, 3029–3039. doi: 10.5194/bg-12-3029-2015

Bostick, K. W., Zimmerman, A. R., Wozniak, A. S., Mitra, S., and Hatcher, P. G. (2018). Production and composition of pyrogenic dissolved organic matter from a logical series of laboratory-generated chars. *Front. Earth Sci.* 6:43. doi: 10.3389/feart.2018.00043

Brodowski, S., John, B., Flessa, H., and Amelung, W. (2006). Aggregate-occluded black carbon in soil. *Eur. J. Soil Sci.* 57, 539–546. doi: 10.1111/j.1365-2389.2006.00807.x

Brodowski, S., Rodionov, A., Haumaier, L., Glaser, B., and Amelung, W. (2005). Revised black carbon assessment using benzene polycarboxylic acids. *Org. Geochem.* 36, 1299–1310. doi: 10.1016/j.orggeochem.2005.03.011

Butnor, J. R., Samuelson, L. J., Johnsen, K. H., Anderson, P. H., González Benecke, C. A., Boot, C. M., et al. (2017). Vertical distribution and persistence of soil organic carbon in fire-adapted longleaf pine forests. *For. Ecol. Manage.* 390, 15–26. doi: 10.1016/j.foreco.2017.01.014

Certini, G. (2005). Effects of fire on properties of forest soils: a review. *Oecologia* 143, 1–10. doi: 10.1007/s00442-004-1788-8

Certini, G., Nocentini, C., Knicker, H., Arfaioli, P., and Rumpel, C. (2011). Wildfire effects on soil organic matter quantity and quality in two fire-prone Mediterranean pine forests. *Geoderma.* 167–168, 148–155. doi: 10.1016/j.geoderma.2011.09.005

Cotrufo, F., Boot, C., Abiven, S., Foster, E. J., Haddix, M., Reisser, M., et al. (2016). Quantification of pyrogenic carbon in the environment: an integration of analytical approaches. *Org. Geochem.* 100, 42–50. doi: 10.1016/j.orggeochem.2016.07.007

Czimczik, C. I., and Masiello, C. A. (2007). Controls on black carbon storage in soils. *Global Biogeochem. Cycles* 21, 1–8. doi: 10.1029/2006GB002798

Czimczik, C. I., Preston, C. M., Schmidt, M. W. I., and Schulze, E. D. (2003). How surface fire in Siberian Scots pine forests affects soil organic carbon in the forest floor: Stocks, molecular structure, and conversion to black carbon (charcoal). *Global Biogeochem. Cycles* 17:1020. doi: 10.1029/2002GB001956

Czimczik, C. I., Schmidt, M. W. I., and Schulze, E. D. (2005). Effects of increasing fire frequency on black carbon and organic matter in Podzols of Siberian Scots pine forests. *Eur. J. Soil Sci.* 56, 417–428. doi: 10.1111/j.1365-2389.2004.00665.x

De La Rosa, J. M., Miller, A. Z., and Knicker, H. (2018). Soil-borne fungi challenge the concept of long-term biochemical recalcitrance of pyrochar. *Sci. Rep.* 8, 1–9. doi: 10.1038/s41598-018-21257-5

Delcourt, H. R., and Delcourt, P. A. (1997). Pre-Columbian native American use of fire, on southern appalachian landscapes. *Conserv. Biol.* 11, 1010–1014 doi: 10.1046/j.1523-1739.1997.96338.x

Dennison, P. E., Brewer, S. C., Arnold, J. D., and Moritz, M. A. (2014). Large wildfire trends in the western United States, 1984–2011. *Geophys. Res. Lett.* 41, 2928–2933. doi: 10.1002/2014GL059576

Department of Energy Office of Science, U. (2009). *Carbon Cycling and Biosequestration Workshop Report*.

Dittmar, T. (2008). The molecular level determination of black carbon in marine dissolved organic matter. *Org. Geochem.* 39, 396–407. doi: 10.1016/j.orggeochem.2008.01.015

Doerr, S. H., Santín, C., Merino, A., Belcher, C. M., and Baxter, G. (2018). Fire as a removal mechanism of pyrogenic carbon from the environment: effects of fire and pyrogenic carbon characteristics. *Front. Earth Sci.* 6:127. doi: 10.3389/feart.2018.00127

Gibson, C., Hatton, P.-J., Bird, J., Nadelhoffer, K., Ward, C., Stark, R., et al. (2018). Interacting controls of pyrolysis temperature and plant taxa on the degradability of PyOM in fire-prone northern temperate forest soil. *Soil Syst.* 2:48. doi: 10.3390/soilsystems2030048

Glaser, B., Haumaier, L., Guggenberger, G., and Zech, W. (1998). Black carbon in soils: the use of benzenecarboxylic acids as specific markers. *Org. Geochem.* 29, 811–819. doi: 10.1016/S0146-6380(98)00194-6

González-Pérez, J. A., González-Vila, F. J., Almendros, G., Knicker, H., Gonzalez-Perez, J., a, Gonzalez-Vila, F. J., et al. (2004). The effect of fire on soil organic matter - a review. *Environ. Int.* 30, 855–870. doi: 10.1016/j.envint.2004.02.003

Hammes, K., Schmidt, M. W. I., Smernik, R. J., Currie, L. A., Ball, W. P., Nguyen, T. H., et al. (2007). Comparison of quantification methods to measure fire-derived (black-elemental) carbon in soils and sediments using reference materials from soil, water, sediment and the atmosphere. *Global Biogeochem. Cycles* 21:GB3016. doi: 10.1029/2006GB002914

Harmon, M. (1982). Fire history of the westernmost portion of Great Smoky Mountains National Park. *Bull. - Torrey Bot. Club.* 109:74doi: 10.2307/2484470

Hatten, J. A., Zabowski, D., Ogden, A., Theis, W., and Choi, B. (2012). Role of season and interval of prescribed burning on ponderosa pine growth in relation to soil inorganic N and P and moisture. *For. Ecol. Manage.* 269, 106–115. doi: 10.1016/j.foreco.2011.12.036

Hatten, J. A., Zabowski, D., Ogden, A., and Thies, W. (2008). Soil organic matter in a ponderosa pine forest with varying seasons and intervals of prescribed burn. *For. Ecol. Manage.* 255, 2555–2565. doi: 10.1016/j.foreco.2008.01.016

Hatten, J. A., Zabowski, D., Scherer, G., and Dolan, E. (2005). A comparison of soil properties after contemporary wildfire and fire suppression. *For. Ecol. Manage.* 220, 227–241. doi: 10.1016/j.foreco.2005.08.014

Heckman, K., Throckmorton, H., Clingensmith, C., González Vila, F. J., Horwath, W. R., Knicker, H., et al. (2014). Factors affecting the molecular structure and mean residence time of occluded organics in a lithosequence of soils under ponderosa pine. *Soil Biol. Biochem.* 77, 1–11. doi: 10.1016/j.soilbio.2014.05.028

Hockaday, W. C., Grannas, A. M., Kim, S., and Hatcher, P. G. (2006). Direct molecular evidence for the degradation and mobility of black carbon in soils from ultrahigh-resolution mass spectral analysis of dissolved organic matter from a fire-impacted forest soil. *Org. Geochem.* 37, 501–510. doi: 10.1016/j.orggeochem.2005.11.003

Huang, W., Hu, Y., Chang, Y., Liu, M., Li, Y., Ren, B., et al. (2018). Effects of fire severity and topography on soil black carbon accumulation in boreal forest of Northeast China. *Forests* 9:408. doi: 10.3390/f9070408

Jaffé, R., Ding, Y., Niggemann, J., Vähätalo, A. V., Stubbins, A., Spencer, R. G. M., et al. (2013). Global charcoal mobilization from soils via dissolution and riverine transport to the oceans. *Science* 340, 345–37. doi: 10.1126/science.1231476

Jolly, W. M., Cochrane, M. A., Freeborn, P. H., Holden, Z. A., Brown, T. J., Williamson, G. J., et al. (2015). Climate-induced variations in global wildfire danger from 1979 to 2013. *Nat. Commun.* 6, 1–11. doi: 10.1038/ncomms8537

Kappenberg, A., Bläsing, M., Lehndorff, E., and Amelung, W. (2016). Black carbon assessment using benzene polycarboxylic acids: limitations for organic-rich matrices. *Org. Geochem.* 94, 47–51. doi: 10.1016/j.orggeochem.2016.01.009

Key, C. H., and Benson, N. C. (2006). "Landscape assessment (LA) sampling and analysis methods," in *FIREMON: Fire Effects Monitoring and Inventory System*. Eds C Duncan, R. E. Keane, J. F. Caratti, C. H. Key, N. C. Benson, S. Sutherland, L. J. Gangi (Fort Collins, CO: USDA For. Serv. Gen. Tech. Re. RMRS- 164-CD).

Lafon, C. W., Naito, A. T., Grissino-Mayer, H. D., Horn, S. P., and Waldrop, T. A. (2017). *Fire History of the Appalachian Region: A Review and Synthesis.* General Technical Report SRS-219. Asheville, NC: U.S. Department of Agriculture, Forest Service, Southern Research Station.

LaForest, L. B. (2012). *Fire Regimes of Lower-elevation Forests in Great Smoky Mountains National Park*, (Ph.D. dissertation). University of Tennessee, Knoxville, TN.

Lehmann, J., and Kleber, M. (2015). The contentious nature of soil organic matter. *Nature* 528, 60–8. doi: 10.1038/nature16069

Lenth, R. V. (2016). Least-squares means: the R package lsmeans. *J. Stat. Softw.* 69, 1–33. doi: 10.18637/jss.v069.i01

Lutfalla, S., Abiven, S., Barré, P., Wiedemeier, D. B., Christensen, B. T., Houot, S., et al. (2017). Pyrogenic carbon lacks long-term persistence in temperate arable soils. *Front. Earth Sci.* 5, 1–10. doi: 10.3389/feart.2017.00096

Major, J., Lehmann, J., Rondon, M., and Goodale, C. (2010). Fate of soil-applied black carbon: downward migration, leaching and soil respiration. *Glob. Chang. Biol.* 16, 1366–1379. doi: 10.1111/j.1365-2486.2009.02044.x

Masiello, C. A. (2004). New directions in black carbon organic geochemistry. *Mar. Chem.* 92, 201–213. doi: 10.1016/j.marchem.2004.06.043

Masiello, C. A., and Druffel, E. R. M. (1998). Black carbon in deep-sea sediments. *Science* 280, 1911–1913. doi: 10.1126/science.280.5371.1911

Masiello, C. A., Kane, E. S., Ohlson, M., Doerr, S. H., Dittmar, T., Preston, C. M., et al. (2015). Towards a global assessment of pyrogenic carbon from vegetation fires. *Glob. Chang. Biol.* 22, 76–91.

Matosziuk, L. M., Alleau, Y., Kerns, B. K., Bailey, J., Johnson, M. G., and Hatten, J. A. (2019). Effects of season and interval of prescribed burns on pyrogenic carbon in ponderosa pine stands in Malheur National Forest. *Geoderma* 348, 1–11. doi: 10.1016/j.geoderma.2019.04.009

McBeath, A. V., Smernik, R. J., Schneider, M. P. W., Schmidt, M. W. I., and Plant, E. L. (2011). Determination of the aromaticity and the degree of aromatic condensation of a thermosequence of wood charcoal using NMR. *Org. Geochem* 42, 1194–1202. doi: 10.1016/j.orggeochem.2011.08.008

National Park Service, US Department of the Interior Division of Fire and Aviation (2017). *Chimney Tops 2 Fire.* Review: Individual Fire Review Report.

Nave, L. E., Vance, E. D., Swanston, C. W., and Curtis, P. S. (2011). Fire effects on temperate forest soil C and N storage. *Ecol. Appl.* 21, 1189–1201. doi: 10.1890/10-0660.1

Pellegrini, A. F. A., Ahlström, A., Hobbie, S. E., Reich, P. B., Nieradzik, L. P., Staver, A. C., et al. (2017). Fire frequency drives decadal changes in soil carbon and nitrogen and ecosystem productivity. *Nature* 553, 194–198. doi: 10.1038/nature24668

Preston, C. M., and Schmidt, M. W. I. (2006). Black (pyrogenic) carbon: a synthesis of current knowledge and uncertainties with special consideration of boreal regions. *Biogeosciences* 3, 397–420. doi: 10.5194/bg-3-397-2006

Reisser, M., Purves, R. S., Schmidt, M. W. I., and Abiven, S. (2016). Pyrogenic carbon in soils: a literature-based inventory and a global estimation of its content in soil organic carbon and stocks. *Front. Earth Sci.* 4:80. doi: 10.3389/feart.2016.00080

Rumpel, C., Chaplot, V., Planchon, O., Bernadou, J., Valentin, C., and Mariotti, A. (2006). Preferential erosion of black carbon on steep slopes with slash and burn agriculture. *Catena* 65, 30–40. doi: 10.1016/j.catena.2005.09.005

Santín, C., Doerr, S. H., Kane, E. S., Masiello, C. A., Ohlson, M., de la Rosa, J. M., et al. (2016). Towards a global assessment of pyrogenic carbon from vegetation fires. *Glob. Chang. Biol.* 22, 76–91. doi: 10.1111/gcb.12985

Santín, C., Doerr, S. H., Preston, C., and Bryant, R. (2013). Consumption of residual pyrogenic carbon by wildfire. *Int. J. Wildl. Fire* 22, 1072–1077. doi: 10.1071/WF12190

Schmidt, M. W. I., and Noack, A. G. (2000). Black carbon in soils and sediments: Analysis, distribution, implications, and current challenges. *Global Biogeochem. Cycles* 14, 777–793. doi: 10.1029/1999GB001208

Schmidt, M. W. I., Torn, M. S., Abiven, S., Dittmar, T., Guggenberger, G., Janssens, I., et al. (2011). Persistence of soil organic matter as an ecosystem property. *Nature* 478, 49–56. doi: 10.1038/nature10386

Schneider, M. P. W., Hilf, M., Vogt, U. F., and Schmidt, M. W. I. (2010). The benzene polycarboxylic acid (BPCA) pattern of wood pyrolyzed between 200°C and 1000°C. *Org. Geochem.* 41, 1082–1088. doi: 10.1016/j.orggeochem.2010.07.001

Schneider, M. P. W., Pyle, L. A., Clark, K. L., Hockaday, W. C., Masiello, C. A., and Schmidt, M. W. I. (2013). Toward a "Molecular Thermometer" to estimate the charring temperature of wildland charcoals derived from different biomass sources. *Environ. Sci. Technol.* 47:11490–11495 doi: 10.1021/es401430f

Schneider, M. P. W., Smittenberg, R. H., Dittmar, T., and Schmidt, M. W. I. (2011). Comparison of gas with liquid chromatography for the determination of benzenepolycarboxylic acids as molecular tracers of black carbon. *Org. Geochem.* 42, 275–282. doi: 10.1016/j.orggeochem.2011.01.003

Singh, N., Abiven, S., Torn, M. S., and Schmidt, M. W. I. (2012). Fire-derived organic carbon in soil turns over on a centennial scale. *Biogeosciences* 9, 2847–2857. doi: 10.5194/bg-9-2847-2012

Soil Survey Staff, Natural Resources Conservation Service, and United States Department of Agriculture (2019). *Web Soil Survey.* Available online at: https://websoilsurvey.sc.egov.usda.gov/ (accessed November 1, 2019).

Soucémarianadin, L., Reisser, M., Cécillon, L., Barr,é, P., Nicolas, M., and Abiven, S. (2019). Pyrogenic carbon content and dynamics in top and subsoil of French forests. *Soil Biol. Biochem.* 133, 12–15. doi: 10.1016/j.soilbio.2019.02.013

Soucémarianadin, L. N., Quideau, S. A., MacKenzie, M. D., Bernard, G. M., and Wasylishen, R. E. (2013). Laboratory charring conditions affect black carbon properties: a case study from Quebec black spruce forests. *Org. Geochem.* 62:46. doi: 10.1016/j.orggeochem.2013.07.005

Thomas, G. W. (1996). "Soil pH and soil acidity," in *Methods of Soil Analysis Part 3: Chemical Methods*, ed D. L. Sparks (Madison, WI: Soil Science Society of America), 475–490.

Thorpe, A. S., Barnett, D. T., Elmendorf, S. C., Hinckley, E. L. S., Hoekman, D., Jones, K. D., et al. (2016). Introduction to the sampling designs of the national ecological observatory network terrestrial observation system. *Ecosphere.* 7:e01627. doi: 10.1002/ecs2.1627

Wiedemeier, D. B., Hilf, M. D., Smittenberg, R. H., Haberle, S. G., and Schmidt, M. W. I. (2013). Improved assessment of pyrogenic carbon quantity and quality in environmental samples by high-performance liquid chromatography. *J. Chromatogr. A* 1304, 246–250. doi: 10.1016/j.chroma.2013.06.012

Zimmermann, M., Bird, M. I., Wurster, C., Saiz, G., Goodrick, I., Barta, J., et al. (2012). Rapid degradation of pyrogenic carbon. *Glob. Chang. Biol.* 18, 3306–3316. doi: 10.1111/j.1365-2486.2012.02796.x

Ziolkowski, L. A., Chamberlin, A. R., Greaves, J., and Druffel, E. R. M. (2011). Quantification of black carbon in marine systems using the benzene polycarboxylic acid method: a mechanistic and yield study. *Limnol. Oceanogr. Methods* 9, 140–149. doi: 10.4319/lom.2011.9.140

Zomer, R. J., Bossio, D. A., Sommer, R., and Verchot, L. V. (2017). Global sequestration potential of increased organic carbon in cropland soils. *Sci. Rep.* 7:15554. doi: 10.1038/s41598-017-15794-8

Conflict of Interest: The authors declare that the research was conducted in the absence of any commercial or financial relationships that could be construed as a potential conflict of interest.